Tutor/s

Dr. Ángel Morales García
*Departament de Ciència de Materials i Química Física.*

Dr. Francesc Illas Riera
*Departament de Ciència de Materials i Química Física.*

Grau de Química

# Treball Final de Grau

**On the C(1s) core level binding energy calculations of MXene carbides. A theoretical approach.**

**Sobre l'energia de lligadura del nivell de core C(1s) de carburs MXene. Una aproximació teòrica.**

Néstor Mauricio García-Romeral González

*(June 2020)*

Universitat de Barcelona

BKC Barcelona Knowledge Campus
Campus d'Excel·lència Internacional

*The roughest roads often lead to the top*

Christina Aguilera

Me gustaría dar las gracias a mis tutores Ángel Morales García y Francesc Illas Riera por acogerme en su grupo de investigación para realizar mi trabajo de final de grado y por ayudarme a lo largo de dicho proyecto. En todo momento me han ayudado lo que han podido, dándome consejos de cómo expresarme y mostrándome la mejor forma de exponer la información. Pero, sobre todo, incentivándome a pensar, enseñándome y echando una mano cuando podían, ya siendo por email o por videollamada. Me siento un privilegiado por haber hecho mi TFG en dicho grupo de investigación, haber aprendido y porque casi el proyecto no se haya visto afectado por la situación del COVID-19. A este virus, no obstante, no le quiero agradecer nada en absoluto.

Por último, quiero darme las gracias a mí mismo por conseguir acabar este trabajo sin haberme cansado de él y no haber perdido el interés. Por haber dedicado tanto tiempo y esfuerzo en algo que de verdad me hacía ilusión.

# REPORT

# CONTENTS

# 1. SUMMARY

One of the latest families incorporated to the group of bidimensional (2D) materials is the low-dimensional transition metal carbides, nitrides and carbonitrides known as MXenes. These materials have generated a great interest in Material Science due to the potential use as catalysts, (bio-) sensors, neural electrodes, ion batteries, water purification, electrochemical capacitors and photodetectors. Such applications are directly related with the surface properties demanding thus exhaustive analysis by using sensitive techniques such as X-ray Photoelectron Spectroscopy (XPS). Essentially, XPS measures core level electron binding energies, constituting a notorious method for accessing to the information of the materials composition. In the present study, first-principles calculations based on the Density Functional Theory (DFT) are employed to investigate C(1s) binding energy of MXenes along with additional parameters such as the charge of carbon atom. In particular, MXene carbides with $M_2C$ stoichiometry (M = Ti, Zr, Hf, V, Nb, Ta, Cr, Mo and W) are selected to this purpose. The goal is to stablish tentative correlation between C(1s) binding energy and the carbon charge that allows one to understand MXenes based on their composition, and the XPS based experiments.

**Keywords**: MXenes, Density Functional Theory, Charge Density, Core Level Binding Energy.

# 2. RESUM

Una de les últimes famílies incorporades al grup de materials bidimensionals (2D) són els carburs, nitrurs i carbonitrurs de metalls de transició de baixa dimensió coneguts com MXenes. Aquests materials han generat un gran interès en la Ciència de Materials degut al potencial ús com a catalitzadors, (bio-) sensors, elèctrodes neurals, bateries d'ions, purificació d'aigua, condensadors electroquímics i fotodetectors. Aquestes aplicacions estan directament relacionades amb les propietats de la superfície que exigeixen una anàlisi exhaustiva mitjançant tècniques sensibles, com ara l'Espectroscòpia Fotoelectrònica de Raigs-X (XPS). Essencialment, l'XPS mesura les energies d'unió d'electrons a nivell de nucli, constituint un mètode notori per accedir a la informació de la composició dels materials. En el present estudi, es fan servir càlculs de primers principis basats en la Teoria del Funcional de la Densitat (DFT) per investigar l'energia d'unió de C(1s) de MXenes juntament amb paràmetres addicionals com la càrrega de l'àtom de carboni. En particular, se seleccionen els carburs de MXene amb estequiometria $M_2C$ (M = Ti, Zr, Hf, V, Nb, Ta, Cr, Mo i W) amb aquesta finalitat. L'objectiu és establir una correlació provisional entre l'energia d'unió de C(1s) i la càrrega de carboni que permeti entendre MXenes en funció de la seva composició i els experiments basats en XPS.

**Paraules clau**: MXenes, Teoria del Funcional de la Densitat, Densitat de Càrrega, Energia d'Unió a Nivell de Nucli.

# 3. INTRODUCTION

Two-dimensional (2D) transition metal carbides, nitrides and carbonitrides, known as MXenes, have gained increasing attention since their discovery, opening new horizons in the 2D world.[1-2] MXenes, with general $M_{n+1}X_n$ chemical formula, have been successfully synthetized by a selective chemical etching of three-dimensional solids known as MAX phases exhibiting a general $M_{n+1}AX_n$ chemical formula, where *M* represents an early transition metal (Sc, Ti, Cr, Y, Zr, Nb, Mo, Ta, Hf or W); *A* stands for an element of the group XIII or XIV, *X* is a carbon and/or nitrogen atom and *n* indicates the sequence in the number of atomic layers (*n*= 1, 2 and 3).[3-4] The first MXene was synthesized in 2011 by separating single $Ti_3C_2$ layers from the $Ti_3AlC_2$ MAX precursor through the selective etching of Al by aqueous hydrofluoric acid (HF) at room temperature.[1,5-6] Alternatively, MXenes can be synthesized from non-MAX phases, like $Mo_2Ga_2C$ that contains two layers of group XIII or XIV atoms separating the carbide layers.[7]

From a synthetic point of view, two steps can be differentiated involving a chemical etching and a mechanical exfoliation (*Figure 1*). The former step corresponds to the selective chemical etching using fluoride-derived agents such as a HF solution, a mixture of HCl and LiF or a $NH_4HF_2$ solution.[6-7] The etchant agents promote the selective breaking of M–A bonds, keeping the M–X bond unaltered. Next, an exfoliation process is applied, which induces the determination of MXenes layers. This step requires traditional methods previously employed in the synthesis of other 2D materials, such as intercalation with large organic molecules, sonication, shaking, and/or intercalation with cations.[6] Due to the usage of etchant and intercalated agents, the as-prepared MXenes surfaces are always functionalized.[4] Fortunately, new protocols have recently been established for cleaning the surfaces generating clean MXenes.[5]

Due to the great variety of MXenes composition, their properties and, consequently, applications are very broad.[6-7,9] Among the properties of interest, we mention electric and ionic conduction, optical, plasmonic and thermoelectric behaviour. These properties make the MXenes good for a wide range of applications, *e.g.*, ion batteries, water purification[6], gas and

energy storage media, electromagnetic interference shielding, reinforcement for composites, gas- and biosensors, lubrication, and electro-, photo- and chemical catalysis. [7,9]

The present study focuses on bare carbide $M_2C$ MXenes, thus composed by three atomic layers ($M_2C$). *Figure 1* shows schematically the selective etching of *A*, *e.g.* with HF, and subsequent chemical exfoliation, leading to MXenes with $M_{n+1}X_n$ formula.[3-4]

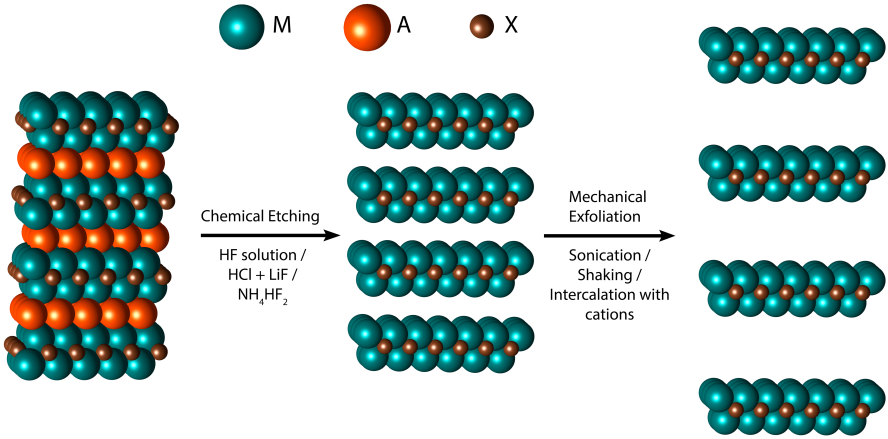


Figure 1. General scheme of the synthesis of MXenes from the MAX phases precursor.

Due to the variability of metal composition of MXenes, it is important to understand the nature of chemical bonding on these systems and which modifications are introduced when going from a metallic element to another. In this sense, X-ray Photoelectron Spectroscopy (XPS) applied to the C(1s) core level emerges as a particularly useful tool to analyse the electronic environment around the C atom and how that changes depending on the early transition metal involved in the MXene. It is worth pointing out that XPS is a widely used analytical technique applicable different types of materials and surface sensivity.[10] XPS is based on Einstein's equation for the photoelectric effect (Eq. 1):

$$h\nu = BE + E_k + \Phi \qquad (1)$$

When the material is irradiated with X-ray of $\nu$ frequency, an electron is ejected with a given, measurable, kinetic energy ($E_k$). In Eq. 1 the electron binding energy and work function are

labelled as BE and $\Phi$, respectively. By definition, in a molecular system, BE corresponds to the energy required to promote an electron from its level to the vacuum. In the case of an infinite solid, BE corresponds to the energy required to promote an electron from its level to Fermi level. Then, an extra energy is needed to bring the electron to the vacuum, and this is precisely the surface work function.[11]

Very briefly, the goal of the present study is to investigate the atomic environment of bare MXene carbides with the stoichiometry $M_2C$ (M= Ti, V, Cr, Zr, Nb, Mo, Hf, Ta, and W) by analysing the C(1s) core level binding energies by using first-principles derived methods. Next, we will try to relate the core level binding energy shift ($\Delta$CLBE) to the topological charge of the C atom in each MXene. The main idea is to investigate to how extent these shifts are correlated to charge transfer effects. In this work, different approximations to the calculation of CLBEs will be used considering initial and final state effects.

# 4. OBJECTIVES

The main goal of this study is to investigate the atomic environment of bare $M_2C$ (M= Ti, V, Cr, Zr, Nb, Mo, Hf, Ta, and W) MXene carbides and to capture trends that allow one to understand details of the chemical bond in these materials. Having this idea in mind, the following properties and their relationship will be discussed in detail:

- Analysis of the topological charge of C atom based on the atoms-in-molecules theory proposed by Bader.
- Analysis of C(1s) core level binding energies (CLBE) using theoretical approaches including initial and final states.
- Identify correlations between the C atom charge and C(1s) ΔCLBEs.
- Make a prediction of CLBEs of C(1s) atom for bare $M_2C$ MXenes.
- Compare the CLBEs with available experimental data.

# 5. THEORETICAL BACKGROUND

## 5.1. QUANTUM MECHANICS

Quantum mechanics is the branch of science that deals with atomic and molecular properties and the behaviour of matter at atomic scale. This theory is in many ways an outstanding "engineering tool" due to its extremely power for understanding and predicting the properties of atoms, molecules and different types of materials. The use of quantum mechanics in the study of microscopic systems goes through the solution of the Schrödinger equation. In general, this is a time dependent equation, although for static properties one can rely on the time-independent version which governs the so-called stationary states.

### 5.1.1. The time independent Schrödinger equation

In order to understand the behaviour of quantum systems, it is necessary to determine the corresponding wavefunction $\Psi$ for every point in the region of interest by solving the time independent Schrödinger equation considering stationary electronic states. The time-independent Schrödinger equation takes the following symbolic form Eq. 2:

$$\hat{H}\Psi = (\hat{T} + \hat{V})\Psi = E\Psi \qquad (2)$$

Where, $\hat{H}$ is the Hamiltonian operator, $\hat{T}$ is the kinetic energy operator, $\hat{V}$ is the potential energy operator, *E* is the energy eigenvalue for the stationary state described by the wavefunction $\Psi$. In order to develop a realistic and useful theory, it is required to describe systems with many electrons and nuclei. Consequently, many electrons and many nuclei together demand a many-body wavefunction, which depends on the positions of each electron and each nucleus in the system. According to this, *E* now represents the total energy of the system in the quantum state specified by the many-body wavefunction.

The kinetic energy is written as in the one-particle scheme but generalized to *N* electrons and *M* nuclei (Eq. 3):

$$\hat{T} = -\sum_i \frac{\hbar^2}{2m_N} \nabla^2(r_i) - \sum_i \frac{\hbar^2}{2m_M} \nabla^2(R_i) \qquad (3)$$

For the potential energy term, we need to take into account the Coulomb interaction between electron pairs (Eq. 4), pairs of nuclei (Eq. 5) and electrons and nuclei (Eq. 6):

$$\hat{V}_{ee} = \sum_i \sum_{j>i} \frac{e^2}{4\pi\varepsilon_0 |r_i - r_j|} \tag{4}$$

$$\hat{V}_{NN} = \sum_i \sum_{j>i} \frac{Z_i Z_j e^2}{4\pi\varepsilon_0 |R_i - R_j|} \tag{5}$$

$$\hat{V}_{Ne} = -\sum_i \sum_j \frac{Z_i e^2}{4\pi\varepsilon_0 |R_i - r_j|} \tag{6}$$

At this point, we can combine the equations (2-6) and write the many-body Schrödinger equation (Eq. 7):

$$\left[ \begin{array}{c} -\sum_i \frac{\hbar^2}{2m_N} \nabla^2(r_i) - \sum_i \frac{\hbar^2}{2m_M} \nabla^2(R_i) + \sum_i \sum_{j>i} \frac{e^2}{4\pi\varepsilon_0 |r_i - r_j|} \\ + \sum_i \sum_{j>i} \frac{Z_i Z_j e^2}{4\pi\varepsilon_0 |R_i - R_j|} - \sum_i \sum_j \frac{Z_i e^2}{4\pi\varepsilon_0 |R_i - r_j|} \end{array} \right] \Psi = E\Psi \tag{7}$$

The solution of this equation provides all the necessary information to predict the behaviour of materials at equilibrium. In addition, finding the eigenstate with the lowest energy (so-called ground state) allows one to predict all equilibrium properties of any system of interest, from elastic properties to enthalpies formation or thermal properties to name a few.[12]

Unfortunately, solving Eq. 7 is extremely challenging, and in most cases, it is still practically impossible. Thus, approximations and simplifications are introduced to be able to use it in practical applications. A first approximation used to solve Eq. 7 is the so-called Born-Oppenheimer Approximation (BOA), that consist in decoupling the electron motion from that of the nuclei which is justified by the fact that the nuclei mass is by far larger than the mass of electrons.[12] Within the BOA, the wavefunction just depends on nuclei positions parametrically, the kinetic energy of nuclei is zero and the repulsion between nuclei and electrons becomes a constant which depends on the nuclear configuration. The BOA approach allows one to

separate the study of the system in two stages: first, solving the electron problem with fixed nuclei positions and later, solving the nuclei issue using the generated solution.[12]

Under the BOA approach, the Schrödinger equation has been reduced to solve the electronic contribution of the Hamiltonian operator (Eq. 8).

$$\hat{H}_{el} = \hat{T}_e + \hat{V}_{ee} + \hat{V}_{eN} \quad (8)$$

Due to the interaction between electrons in a polyelectronic systems, solving Eq. 8 becomes also challenging and still constitutes a many-body problem. Two main approximations have been broadly used, both relying on the variational principle. These are the Hartree-Fock (HF) method and the Density Functional Theory (DFT). The Hartree-Fock (HF) method aims at providing the best approximation to the N-electron wavefunction that can be written as a single Slater determinant. This is intrinsically an independent particle model where the electron-electron interaction is taken as an average. In particular, it can be shown that the correlation energy between electrons of opposite-spin electrons is not taken into account.[13] To solve this many-body problem, several methods have been developed, *e.g.* Configuration Interaction (CI) methods, which is based on expanding the wavefunction as a linear combination of Slater determinants.[14] The resulting methods are generically referred to as wavefunction based methods and have the common feature of being computationally demanding. Alternatively, the DFT based methods provides a different way to solve the Schrödinger equation for the electronic ground state of any polyelectronic system without needing to refer to its wavefunction. Instead, the ground state energy of the system is determined by its one electron density only. Consequently, the computational cost of DFT is much less than computational cost of wavefunction based methods, HF, and thus DFT is especially well-suited for the study of surface or bulk materials.[15]

### 5.1.2. Density Functional Theory (DFT)

As mentioned in the previous section, determining the quantum states of a system with *N* electrons is highly expensive computationally because it involves 4*N* dimensions (3 spatial and one of spin) in the many-body wavefunction.[16]

The core of density functional theory (DFT) relies on Hohenberg and Kohn's theorems published in 1964.[17] The first theorem states that the energy of non-degenerated ground state, $E_o$, is given by a universal functional just of the electron density, $\rho(r)$, (Eq. 9).

$$E_o = E_o[\rho(r)] \tag{9}$$

This observation is quite remarkable since it implies that the energy of the electronic ground state –in principle a functional of the whole *N*-electron wavefunction depending on 4*N* variables– can be obtained from a function depending only on three spatial variables. The second theorem is based on the variational method. This theorem establishes that the energy of a non-degenerate ground state can be obtained variationally and that the density that minimizes the total ground state energy is, indeed, the exact electron density of said non-degenerate ground state (Eq. 10), and when $\rho(r)$ coincides with the electron density of the ground state, $\rho_o(r)$, the resulting energy is the exact energy of the ground state.

$$E_o \leq E[\rho(r)] \tag{10}$$

These Hohenberg and Kohn's theorems establish three premises: (i) the electron density is determined by uniquely the external potential ($V_n$, which is the nuclei-electron potential in Eq. 8); (ii) $V_n$ determines exclusively the ground state many-electron wavefunction; and finally (iii) the ground state total energy, *E*, which is a functional of the many-body wavefunction through $E = \langle \Psi | \hat{H} | \Psi \rangle$, becomes a functional of the density only; *i.e.* $E = E[\rho(r)]$, where $\rho(r)$ is defined as in Eq. 11, its integral through the volume must be the number of electrons (Eq. 12) and its value tends to zero as the distance increases (Eq. 13).[14, 16-17]

$$\rho(r) = N \int \dots \int \left|\Psi(x_1, x_2, \dots, x_n)\right|^2 dx_1 dx_2 \dots dx_n \tag{11}$$

$$\int \int \int \rho(r) dV = N \tag{12}$$

$$\lim_{r \to \infty} \rho(r) = 0 \tag{13}$$

The electron density function in Eq. 11 provides the probability of finding an electron with arbitrary spin in a determined volume independently of the position and spin of the rest of electrons.

As explained above, the Hohenberg-Kohn's theorem stablishes that the total energy of many electrons in their ground state is provided by a universal functional of the electron density. However, it does not provide any clue about how to construct such universal functional. Therefore, to be of practical use, DFT needs further approximations. Here, the so-called Kohn-Sham's (KS) equations come into play. In particular, the KS approximation specifies that, for a given external potential, a fictious system of independent (non-interacting) electrons exists in such a way that its density, $\rho(r)$, is equal to that of the system of interest.[14] This hypothesis allows one to derive a set of equations that are similar to those corresponding to the HF methods. These are known as the Kohn-Sham equations and are given by Eq. 14 and 15.

$$\left[\frac{-\hbar^2}{2\mathrm{m}}\nabla^2+\mathrm{v_s}[\rho_o](\mathrm{r})\right]\varphi_\mathrm{i}(\mathrm{r})=\varepsilon_\mathrm{i}\varphi_\mathrm{i}(\mathrm{r}) \tag{14}$$

$$\rho_o(r) = \sum_i^N|\varphi_\mathrm{i}(\mathrm{r})|^2 \tag{15}$$

Where $\mathrm{v_s}(r)$ is the local effective (fictitious) potential determining the electronic density, usually known as Kohn-Sham potential; $\varepsilon_\mathrm{i}$ is the eigenvalue that represents the orbital energy of the corresponding Kohn-Sham orbital, $\varphi_\mathrm{i}(\mathrm{r})$, and $\rho_o(r)$ is the electronic density for the *N*-particle system.[14] It is important to realize that, except for electron density, the terms in Eq. 14 and 15 are physically meaningless. The whole idea of the KS approach is to provide a form for the electron density that allows one to compute the total energy from it. In fact, the kinetic energy of the independent electron system, the potential energy from the nuclei-electron external potential and the classical Coulomb interaction between electrons can be easily obtained from the electron density only (see Eq. 16). Clearly, there are missing terms like the contribution to the kinetic energy due to the electrons' interaction, the exchange and correlation terms which also come from the fact that the electrons interact. All the missing terms are collected on the so-called exchange-correlation energy which must depend on the density only (*i.e.* $E_{xc}[\rho(r)]$).[14,15]

$$E = T_s[\rho(r)] + V_{Ne}[\rho(r)] + J[\rho(r)] + E_{xc}[\rho(r)] \quad (16)$$

Where $T_s$ is the kinetic energy of the fictitious system electrons; $V_{Ne}$, attraction energy of the electrons to pseudopotential; $J$, repulsion energy between electrons and a new term labelled as $E_{xc}$, the exchange correlation energy that includes: the correlation energy and exchange energy of electrons and the difference of kinetic energy of the system studied and the fictional system.[14-15] The remaining question is, therefore, how to actually determine the $E_{xc}$.

The $E_{xc}$ can be calculated through Eq. 17, where $T_k(\rho)$ is the kinetic energy of the real system and $V_{ee}(\rho)$ the repulsion energy between electrons in the real system.

$$E_{xc}(\rho) = T_k[\rho(r)] - T_s[\rho(r)] + V_{ee}[\rho(r)] - J[\rho(r)] \quad (17)$$

Obviously, this is not a practical way to proceed as both $T_k$ and $V_{ee}$ are unknown. This is why exchange-correlation functionals are needed that are described in the following section.

### 5.1.3. The exchange correlation energy and potential

Since the introduction of the Kohn-Sham's theory, a huge effort has been devoted to deriving accurate exchange and correlation functionals, $E_{xc}(\rho)$, in order to solve the Kohn-Sham equations that are formally equivalent to those in Eq. 14. Note that the potential does not correspond to that of the independent electron system, but it is that of the real system. It can be shown that the Kohn-Sham equations are obtained when minimizing the energy as given in Eq. 16 and that the corresponding potential is the functional derivative of the $E_{xc}(\rho)$ in Eq. 17. The $E_{xc}(\rho)$ term is a functional of the electronic density[14] where some of the energy contributions are unknown. Consequently, the energy in Eq. 16 cannot be obtained unless some form is chosen for the $E_{xc}(\rho)$ functional. There are basically several different approaches to the unknown exchange correlation (xc) functional: these are the so-called Local Density Approximation (LDA), the Generalized Gradient Approximation (GGA) those grouped under the meta-GGA term and the family of hybrid functionals.

The simplest approach is that provided by the Local Density Approximation (LDA). It assumes that the first derivate of the electronic density of the ground state respect the position

is approximately zero, (Eq. 18), *i.e.* the electronic density of the ground state is constant along the space. Then, the xc functional only depends on the electron density (Eq. 19).[14]

$$\frac{\partial \rho_o(r)}{\partial r} \approx 0 \tag{18}$$

$$E_{xc}[\rho(r)] = \int f[\rho(r)]\, dr \tag{19}$$

The second one is, nowadays broadly used, Generalized Gradient Approximation (GGA). The electron density of any real system is not spatially homogeneous, there is a variation in density along the space, GGA approximately includes this variation in such a way that the xc functional depends on the electron density at each point of the space and on the density gradient $\nabla\rho(r)$ as in Eq. 20.[14] *e.g.* Perdew–Burke–Ernzerhof (PBE)[18]. In this work, PBE xc functional is selected to carry out the calculations.

$$E_{xc}[\rho(r)] = \int f[\nabla\rho(r), \rho(r)]\, dr \tag{20}$$

The meta-GGA functionals aim to go one step further in the expansion of the electron density and include the Laplacian of the density, $\tau(r)$, to xc functional as in Eq. 21.[14]

$$E_{xc}[\rho(r)] = \int f[\nabla\rho(r), \rho(r), \tau(r)]\, dr \tag{21}$$

Finally, hybrid functionals, which was introduced to provide an accurate description of thermochemistry of gas phase molecules, include a fraction of the non-local Hartree-Fock exchange to xc functional; the broadly used PBE0 and B3LYP methods make use of hybrid xc functionals.[14]

## 5.2. PERIODIC MODELS

There are two ways to represent a solid material through periodic or cluster models. Both are idealized models and the choice of one or the other depends on the system and/or properties to be studied. In the cluster models, a section of the material is cut from the bulk

containing the region of interest, whereas in the periodic approach the system is assumed to be a perfect, infinite crystal with periodic symmetry. The crystalline bulk materials are designed by accounting symmetry properties as convenient representation[19] although clusters models may be more suitable to dealing with point defects and excited states.[20]

Periodic models start from the so-called unit cell, which reproduces a perfect and infinite crystal by periodic symmetry in the three directions of the space. Consequently, the use of periodic symmetry allows one to reduce significantly the computational cost of calculating the DFT (or HF) energy of a certain material with a large number of atoms and electrons just having to consider the atoms within the unit cell. Although, a detailed analysis shows that the situation is not that idyllic since one needs to solve the corresponding Kohn-Sham's (or HF) equations in a representative number of points in the reciprocal space. In the particular case of MXenes, and due to its bidimensional nature, the use of a fully periodic approach is reasonable. In addition, it requires including 10 Å of vacuum in the perpendicular direction to the surface material to avoid interaction between the periodic replicas (*Figure 2*).

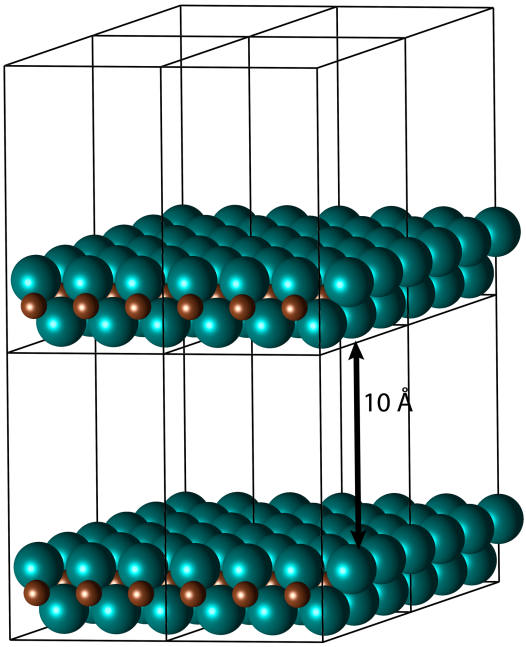


Figure 2. Replicated unit cell of a generic $M_2C$ MXene including a 10 Å of vacuum to properly simulate this two-dimensional material.

## 5.3. ATOMIC CHARGES FROM QUANTUM THEORY OF ATOMS IN MOLECULES (QTAIM)

The topological analysis based on the Quantum Theory of Atom-In-Molecules (QTAIM) provides a well-defined framework to estimate atomic charges in molecules that can be used to calculate atomic charges in solids.[21] In a finite system, the electrons distribute themselves through the space in an external attractive field generated by nuclei, also named attractors. This is because a topological analysis of $\rho(r)$ show that the position of the nuclei corresponds to maxima of $\rho(r)$. The same analysis shows that there is a region in space where the gradient of $\rho(r)$ becomes zero and that the surface of zero electron density gradients contain just one attractor. This allows one to define atomic basin as those included inside the zero-electron density surface containing one attractor (nuclei). Integration of the electron density inside the atomic basis provides an unambiguous way to estimate the electron density that is associated to one atom and, hence, to define atomic charges which are usually referred to as Bader charges.[22]

## 5.4. ELECTRON BINDING ENERGIES

The binding energy (BE) of an electron in a system is obtained from the difference between the total energy of the neutral state with *N* electrons and the same system with a core hole configuration generated by subtracting an electron from the desired core level, *N-1* electrons (Eq. 22).[23]

$$BE = E^{N-1}(final\ system) - E^{N}(intial\ system) \qquad (22)$$

In the case of core electrons, the BE is characteristic of each chemical element and provides the basis for its use as an analytical method. The technique used to measure core level BEs (CLBEs) is the X-Ray Photoelectron Spectroscopy (XPS), as mentioned in the Introduction section. For a given chemical element in different environments, the quantity of special interest is not the core level binding energy (CLBE) absolute value but its shift (ΔCLBE) with respect to a given reference. The analysis of ΔCLBE is broadly used in order to extract information about the local environment of the atom from which the electron is removed and then, it can be used to identify functional groups and oxidation states. Note that these shifts minimise or avoid the error in xc functional and error introduced in PAW method used in the calculations.[11]

Both, CLBEs and ΔCLBEs, are provided by experiments but these quantities can also be obtained from appropriate total energy calculations following Eq. 22. The calculated values can then be used to investigate trends. There are two main approaches to obtain the CLBEs that are denoted as Initial State (IS) and Final State (FS).

In the IS, one considers that the core ionization is extremely fast, then, that the except for the removal of the core electron, the electron density of the *N-1* system has not changed. In other words, the energies in Eq. 22 can be obtained from the same set of orbitals, so-called frozen orbitals. However, in the FS state approach, one accounts for the electron density relaxation effect in response to presence of the core hole.[24] The distinction between IS and FS state effect is important because it is what justifies using XPS to extract information of the neutral system.[24] Even if IS computed CLBEs neglect relaxation of core-electrons on ionization,[11] they normally dominate the ΔCLBEs.[25] This is because the effects are already present in the neutral system.[24]

In the framework of HF, IS effects are accounted for by the orbital energies through the Koopmans' theorem.[10] In the case of DFT, the Kohn-Sham orbital energies of the electronic ground state do not approach the CLBEs but it has been shown that they are able to provide a reasonable estimate of ΔCLBE.[25] In the implementation of DFT used in the present work with the electron density expanded in a plane wave basis sets and atomic cores replaced by a potential derived from the Projector Augmented Wave (PAW) method,[26] some remarks are necessary, especially regarding the estimate of FS effects. The use of a PAW representation of the atomic cores can be regarded as an effective method in which atomic cores are frozen and a core hole on a determinate level core is generated; the IS CLBE are obtained from the orbital energies provided by the PAW. Afterwards, FS CLBEs can be estimated by generating a core excited ionic PAW which is generated on the fly in the course of the corresponding calculation. However, there is evidence that the differences of Kohn-Sham core level energies taken with respect to a common reference provides a proper way to define the initial state contributions to the ΔCLBE.[25,27]

In the present work, FS effects will be investigated using the different approximation methods following the scheme in *Figure 3*. In these approaches, one attempts to include the relaxation of the electron density around the ionized atom explicitly.[27] Note that in those denoted as *fs* and *JS* (for Janak-Slater) one or half electron, respectively, is promoted from the core level

to the conduction band, respectively.[10-11] This is to avoid dealing with a charged unit cell and this method is only a mathematical device and does not have any physical implications.[28] In the two rightmost methods in *Figure 3* (*fs*$^n$ and *JS*$^n$) one or half electron, respectively, is promoted from the core level and placed conceptually in the vacuum, the charge in the unit cell is compensated by a uniform potential background.[10]

*Figure 3* illustrates the different approaches used to include final state effects.

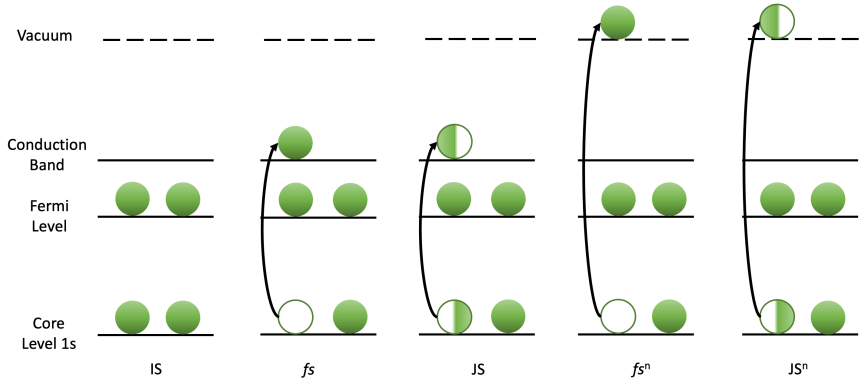


Figure 3. Scheme of the promotion of (half) electron from core level 1s using the approaches IS, *fs*, JS, *fs*$^n$ and JS$^n$.

## 5.5. THE SURFACE WORK FUNCTION

The work function, $\phi$, of a solid material is defined as the energy necessary to promote an electron from Fermi Level to the vacuum and it is specific for each material and each particular surface (Eq. 23).[29] This concept is shown in *Figure 4*.

$$\phi = V - E_{Fermi} \tag{23}$$

Where $E_{Fermi}$ is the Fermi level energy and $V$ is the potential energy in the vacuum. The jellium model by Lang and Kohn[27] was the first to predict the existence of a surface dipole at the surface of any metallic solid material and hence, the physics behind the work function. The fact that the electronic density spills over the surface provoking a superficial dipole implies that a

free electron still needs additional energy to leave the surface towards the vacuum, this is the physical origin of the experimentally measured surface work function.[29-30]

Following Einstein's equation (Eq. 1) on XPS and (Eq. 23) it is possible to construct a mental scheme, and this can be seen in *Figure 4*.

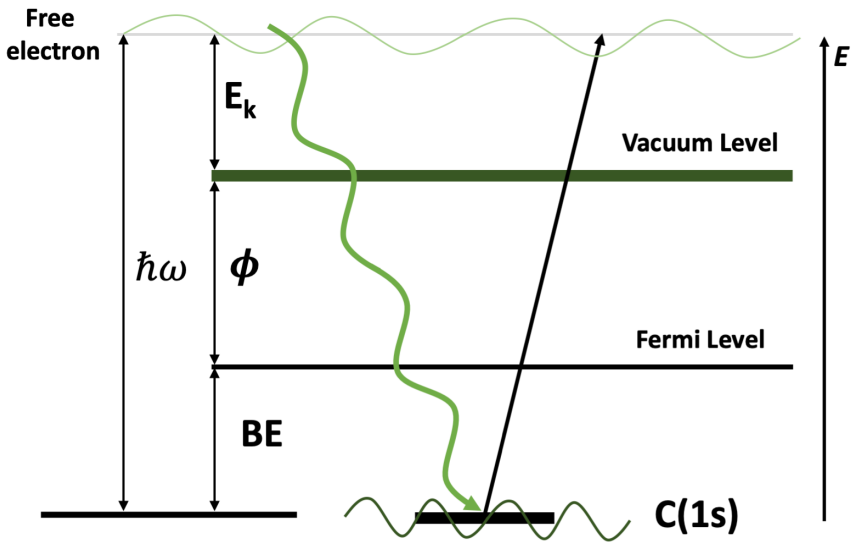


Figure 4: Diagram of the energy levels: C(1s) core level binding energy, Fermi level and vacuum and the energy relations between each of them.

Strictly speaking, the core level binding energies should be referred to the vacuum and this is why the work function is needed. In practice, surface work function is changing constantly during the measurement, just because electrons are ejected from the surface due to the incoming X-ray radiation. It is also usually to use an electron gun to neutralize the sample. Therefore, the measurements are referred to the Fermi level of the analyzer which matches that of the sample since both are in electric contact. Most often, absolute values are calibrated with respect to a well-known peak taken as reference.

# 6. COMPUTATIONAL DETAILS

In order to investigate the trends in the C(1s) core level binding energy (CLBE) of MXenes, first-principles periodic spin-polarized DFT based calculations are performed on suitable surface models. In particular, we consider the most stable $M_2C$ (0001) surfaces – M = Ti, Zr, Hf, V, Nb, Ta, Cr, Mo, and W of these two-dimensional systems. A vacuum of 10 Å in included to avoid the interaction between the replicas.

All calculations are carried out using the *Vienna ab initio Simulation Package* (VASP), employing the Perdew-Burke-Ernzerhof (PBE)[19] implementation of the Generalized Gradient Approximation (GGA) to the exchange-correlation potential. The Kohn-Sham's equations are solved in a plane-wave basis set with a kinetic energy cut-off of 415 eV, high enough to consider the results converged with the basis set within 1 meV. The Projector-Augmented Wave (PAW) method is included to account for the interaction between the valence and the core electron densities.[26] Numerical integrations in reciprocal space are carried out using a Monkhorst-Pack grid of 5 x 5 x 1 special ***k***-points. The geometry optimizations are considered converged when the forces acting on the nuclei are all below 0.01 $eV \cdot Å^{-1}$.

Once the optimized MXene structures have been obtained, the C(1s) CLBE is analyzed by using the different approaches mentioned earlier. The present approach to the initial state (IS) contributions just involves the analysis of the KS eigenvalues of the core states. On the other hand, the final state (FS) is estimated based on the four different approaches (*fs*, JS, $fs^n$ and $JS^n$) already commented, which include, in an approximated way, the relaxation of the electron density in response to the presence of the core hole. In the *fs* and $fs^n$ approaches, the selected electron is promoted to the conduction band or vacuum, respectively; whereas in the JS and $JS^n$ approaches half electron is promoted to conduction band or the vacuum. Even more important than the absolute values of the CLBEs are their shifts, labelled as ΔCLBEs, since they provide information of the differences between similar systems. In the present work, the ΔCLBEs are given relative to graphene. Finally, the QTAIM method[21] is used to calculate the net charges (Bader Charges) of the carbon atom in MXenes.

# 7. RESULTS AND DISCUSSION

The goal of this study is to investigate the atomic environment of bare (0001) $M_2C$ MXene surfaces and to capture meaningful trends that allow one to understand the details of the chemical bonding of these carbide derived materials. To this purpose, the atomic charges taken from the QTAIM analysis and C(1s) CLBEs are separately analysed along with suitable correlation between them.

## 7.1. ATOMIC CHARGES FROM QTAIM ANALYSIS

The atomic charge of C, Q(C), of the investigated MXene carbides are compiled in *Table 1*. Note that the C atom gains electrons depending on the MXene composition, as expected from simple chemical arguments. Interestingly, the C atom of $d^2$ - (Ti, Zr, Hf) MXenes exhibits the largest charge followed by $d^3$ - (V, Nb, Ta) and, finally, the $d^4$ - (Cr, Mo, W) that has the lowest electron´s earning.

| M atom Group | MXene | Q(C) / e | EN (M) / Pauling units[31] |
|---|---|---|---|
| **$d^2$** | **$Ti_2C$** | -2.4 | 1.54 |
| | **$Zr_2C$** | -2.2 | 1.33 |
| | **$Hf_2C$** | -2.5 | 1.30 |
| **$d^3$** | **$V_2C$** | -2.0 | 1.63 |
| | **$Nb_2C$** | -1.9 | 1.60 |
| | **$Ta_2C$** | -2.2 | 1.50 |
| **$d^4$** | **$Cr_2C$** | -1.7 | 1.66 |
| | **$Mo_2C$** | -1.6 | 2.16 |
| | **$W_2C$** | -1.4 | 2.36 |

Table 1. Atomic charge of C atom calculated using QTAIM and electronegativity of M atom in $M_2C$ MXenes.

Moving through the periods of transition metals, the metals' electronegativity increases, consequently, the negative charge accumulated on the C atom decreases in this way. To

exemplify this argument, the Q(C) is -2.35, -2.04, and -1.66 |e| for $Ti_2C$, $V_2C$, and $Cr_2C$, respectively. Nevertheless, variations through the group progression do not allow to determinate systematic trends in that way.

## 7.2. CORE LEVEL C(1S) BINDING ENERGIES ANALYSIS

The C(1s) binding energies (BEs) of MXenes are estimated by using different approaches as described earlier in the subsection 5.4. The CLBE absolute values normalized to the Fermi level of each particular MXene are collected in *Table 2*.

| M atom Group | MXene | CLBE IS / eV | CLBE *fs* / eV | CLBE JS / eV | CLBE $fs^n$ / eV | CLBE $JS^n$ / eV |
|---|---|---|---|---|---|---|
| $d^2$ | $Ti_2C$ | 265.1 | 312.7 | 290.0 | 313.7 | 290.3 |
| | $Zr_2C$ | 265.2 | 312.5 | 289.9 | 313.3 | 290.3 |
| | $Hf_2C$ | 265.0 | 312.6 | 289.8 | 312.9 | 290.1 |
| $d^3$ | $V_2C$ | 265.5 | 313.3 | 290.6 | 314.8 | 291.1 |
| | $Nb_2C$ | 266.1 | 313.6 | 290.5 | 314.8 | 291.1 |
| | $Ta_2C$ | 265.8 | 313.8 | 290.9 | 314.7 | 291.4 |
| $d^4$ | $Cr_2C$ | 265.8 | 313.4 | 290.6 | 314.6 | 291.2 |
| | $Mo_2C$ | 266.6 | 314.1 | 291.4 | 315.1 | 291.4 |
| | $W_2C$ | 266.4 | 313.9 | 291.2 | 314.9 | 291.7 |

Table 2. C(1s) binding energies of $M_2C$ MXenes calculated as Initial State (IS); Final State (*fs*); Janak-State (JS); Final State ($fs^n$) and Janak-Slater ($JS^n$) placing the electron conceptually in the vacuum for *fs* and $fs^n$ and the half electron for JS and $JS^n$, respectively.

Analyzing the C(1s) BEs, it is shown that the $d^2$ - (Ti, Zr, Hf) composed MXenes have lower binding energies than $d^3$ - (V, Nb, Ta) ones, whereas the $d^4$ - (Cr, Mo, W) ones expose the largest energies. This trend is observed regardless the approach used to estimate the C(1s) CLBE. Note that the IS approximation reports systematically lower BEs than the FS approximation due to the later approach take in account the local relaxation effect. Note also that precisely because of this fact, the IS KS values cannot be taken as a measure of the CLBEs, adding relaxation necessarily must decrease the CLBEs, not to increase it. This has been described at length in Refs. 25 and 26. Nevertheless, the focus of the present work in on the trends in the CLBEs along the series rather than on the absolute values. Interestingly, the

trends in CLBEs are similar to those discussed for the Q(C) indicating a correlation between C(1s) BE and Q(C). This will be discussed in the following subsection.

Regarding the absolute values of the CLBEs, it is important to point out that XPS measurements are referenced to the Fermi level of the analyzer rather than to the vacuum as mentioned in section 5.5. This is because the analyzer's work function changes depending on the surface investigated. In practice, the XPS measurements are be calibrated relative to the well-known peaks, *i.e.* taking 285 eV for C(1s).[32]

## 7.3. CORRELATION BETWEEN C(1S) CLBES AND Q(C)

As mentioned above, DFT has limitations in the prediction of accurate CLBEs. However, shifts with respect to a given reference have been shown to be reliable.[25] The ΔCLBEs are useful to extract information about the local environment of the atom from which the electron is removed as identifying functional groups and oxidation states minimizing, or even avoiding, the error induced by the exchange-correlation functional and the representation of the atomic cores through the PAW method.[11]

In the present study, the ΔCLBEs have been calculated considering graphene phase as a reference material. The C(1s) CLBEs corresponding to the IS and the FS states are listed in *Table 3*. Again, these values are referenced to the graphene's Fermi Level. The selection of graphene as reference material is based on its low dimensional morphology analogous to the carbon layer observed in MXene derived materials. Combining *Tables 2* and *3*, the C(1s) ΔCLBE are listed in *Table 4* for the initial and final states along with the Q(C) for all investigated MXenes.

| Material | CLBE IS / eV | CLBE *fs* / eV | CLBE JS / eV | CLBE $fs^n$ / eV | CLBE $JS^n$ / eV |
|---|---|---|---|---|---|
| **Graphene** | 265.7 | 314.5 | 291.3 | 316.5 | 292.2 |

Table 3. Calculated C(1s) CLBEs of graphene phase.

| M atom Group | MXene | Q(C) / e | ΔCLBE IS / eV | ΔCLBE *fs* / eV | ΔCLBE JS / eV | ΔCLBE $fs^n$ / eV | ΔCLBE $JS^n$ / eV |
|---|---|---|---|---|---|---|---|
| $d^2$ | $Ti_2C$ | -2.4 | -0.6 | -1.8 | -1.3 | -2.8 | -1.9 |
| | $Zr_2C$ | -2.2 | -0.5 | -2.0 | -1.4 | -3.2 | -1.9 |
| | $Hf_2C$ | -2.5 | -0.7 | -1.9 | -1.5 | -3.6 | -2.1 |
| $d^3$ | $V_2C$ | -2.0 | -0.2 | -1.2 | -0.7 | -1.7 | -1.1 |
| | $Nb_2C$ | -1.9 | 0.4 | -0.9 | -0.8 | -1.7 | -1.1 |
| | $Ta_2C$ | -2.2 | 0.1 | -0.7 | -0.3 | -1.8 | -0.8 |
| $d^4$ | $Cr_2C$ | -1.7 | 0.1 | -1.1 | -0.6 | -1.9 | -1.0 |
| | $Mo_2C$ | -1.6 | 0.9 | -0.4 | 0.1 | -1.4 | -0.8 |
| | $W_2C$ | -1.4 | 0.7 | -0.6 | -0.1 | -1.6 | -0.5 |

Table 4. Calculated Q(C) and ΔCLBE for each MXene and approach: Initial State (IS); Final State (*fs*); Janak-State (JS); Final State ($fs^n$) and Janak-Slater ($JS^n$).

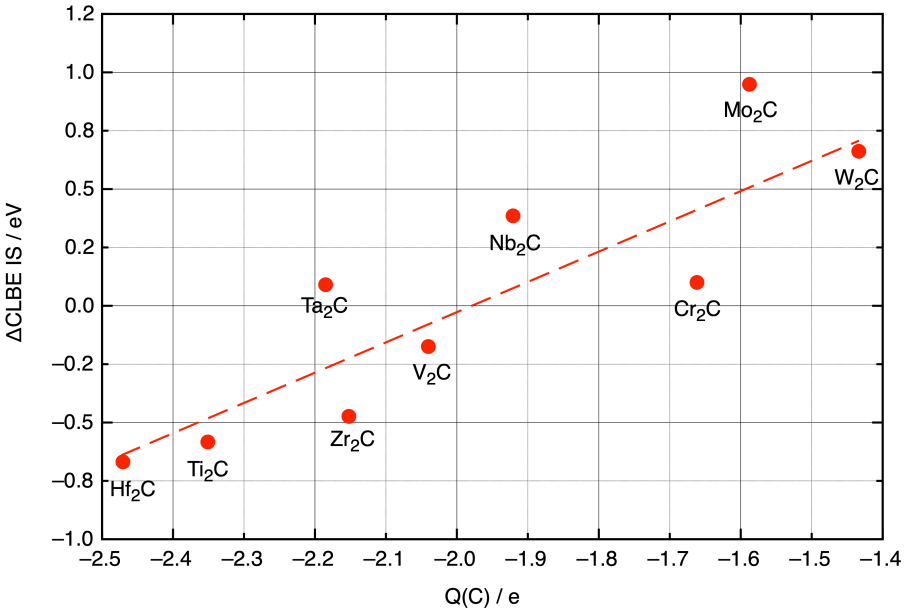


Figure 5. Evolution of ΔCLBEs versus Q(C) for the initial state (IS) compiled in *Table 4*.

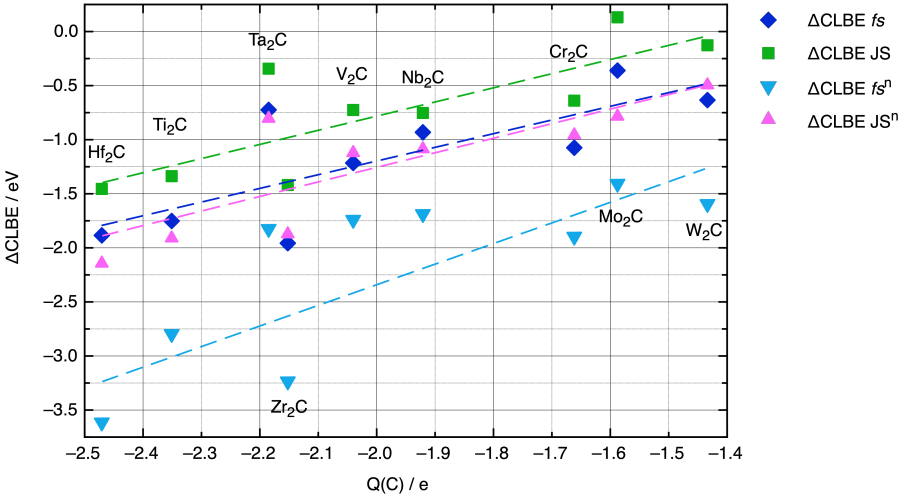


Figure 6. Representation of ΔCLBEs versus Q(C) for Final States: *fs*, JS, *fs*$^n$ and JS$^n$ compiled in *Table 4*.

| Trend line | a / eV/e | b / eV | $R^2$ |
|---|---|---|---|
| **BE IS** | 1.39 | 2.78 | 0.77 |
| **BE *fs*** | 1.26 | 1.31 | 0.59 |
| **BE JS** | 1.30 | 1.83 | 0.65 |
| **BE *fs*$^n$** | 1.74 | 1.24 | 0.60 |
| **BE JS$^n$** | 1.38 | 1.48 | 0.70 |

Table 5. Linear fitting parameters (y=ax+b) corresponding to the IS and FS depicted in *Figures 5* and *6*, respectively.

Looking at *Figure 5*, where calculated C(1s) ΔCLBE of the initial state is represented versus Q(C), a clear correlation between both quantities emerges with a linear fitting $R^2$ coefficient of 0.77, see *Table 5*. This is a clear indication of the C(1s) ΔCLBEs are related to the Q(C) as expected from the fact that the charge is one of the leading mechanisms governing the ΔCLBEs.[24] *Figure 6* shows a similar trend for calculations including the final state contribution. However, it is shown that *fs* and *fs*$^n$ approaches have lower correlation coefficient $R^2$, close to 0.60, than JS and JS$^n$ approaches. Finally, the JS$^n$ approach to the final state has a correlation coefficient similar to the abovementioned IS one.

The fact that the best trend between ΔCLBEs and Q(C) is found for IS implies that the obtained information corresponds to the neutral system, before ionization and relaxation. This is an important, often disregarded, conclusion which validates the use of XPS to get information

about the neutral ground state of materials and surfaces. On the other hand, the FS trends considers the relaxation effect, corresponding to the system post ionized, the relaxed system. From a more technical point of view, note that in the $fs^n$ and $JS^n$ calculations the charge in the unit cell is compensated by a uniform potential background, whereas *fs* and JS approaches consider relaxation energy due to a local response for a core hole generated by subtracting the (half) electron. The approximations behind these methods contribute to a worse correlation between ΔCLBE and Q(C). A much better correlations is to be expected from ΔSCF calculations where the energy of neutral and ionized state is obtained variationally.[24]

## 7.4. PREDICTION OF C(1S) CLBES IN $M_2C$ MXENES

There is strong evidence that IS CLBEs calculated under DFT framework are systematically underestimated respect to the experiments.[25] This is because KS orbital energies do not represent ionization potentials as in the Hartree-Fock theory where Koopman's theorem is fulfilled. However, since the ΔCLBEs are well predicted, it makes sense to attempt to estimate the CLBE values by adding the average relaxation final state contributions. *Table 6* reports such a prediction by taking into account that the average difference between CLBE JS and CLBE IS, 24.9 eV, the later value has been added to CLBE IS values to provide values that would better be compared to experimental data. Note that the predictions from *fs* and JS approaches differ significantly, the latter being in the range of experimental values. This also suggest that the *fs* approaches are not reliable, this is not surprising since one electron is promoted from the core to the conduction band rather than to the continuum.

| M atom Group | MXene | CLBE IS / eV | CLBE *fs* / eV | CLBE JS / eV | CLBE $fs^n$ / eV | CLBE $JS^n$ / eV |
|---|---|---|---|---|---|---|
| $d^2$ | $Ti_2C$ | 290.0 | 312.7 | 290.0 | 313.7 | 290.3 |
| | $Zr_2C$ | 290.1 | 312.5 | 289.9 | 313.3 | 290.3 |
| | $Hf_2C$ | 289.9 | 312.6 | 289.8 | 312.9 | 290.1 |
| $d^3$ | $V_2C$ | 290.4 | 313.3 | 290.6 | 314.8 | 291.1 |
| | $Nb_2C$ | 291.0 | 313.6 | 290.5 | 314.8 | 291.1 |
| | $Ta_2C$ | 290.7 | 313.8 | 290.9 | 314.7 | 291.4 |
| $d^4$ | $Cr_2C$ | 290.7 | 313.4 | 290.6 | 314.6 | 291.2 |
| | $Mo_2C$ | 291.5 | 314.1 | 291.4 | 315.1 | 291.4 |
| | $W_2C$ | 291.3 | 313.9 | 291.2 | 314.9 | 291.7 |

Table 6. Correction of C(1s) CLBE IS on basis of the average Δ(JS-IS).

## 7.5. COMPARISON OF C(1S) CLBES OF $M_2C$ MXENES WITH THE AVAILABLE DATA

Following the previous correction of the IS C(1s) CLBE values (see *Table 6*), a plausible comparison is discussed considering available experimental values obtained from XPS spectra. Recently, XPS based analysis have been reported for $Ti_2CT_x$, $Mo_2CT_x$, $V_2CT_x$, and $Nb_2CT_x$. Note that these synthetized MXenes are functionalized by $T_x$ (F, O, H or OH), but the stoichiometry $M_2C$ is analogous to our models. In *Table 7*, the experimental and calculated C(1s) CLBEs are listed for comparison. The trend between both set of data matches quite well, confirming that the CLBEs previously discussed compare well with experiments thus validating the physical origin of those shifts that are largely due to the charge in the atoms. The observed deviations can be assumed to the presence of terminations in the experimental samples respect to our bare models. Hence, it is expected that an analysis of functionalized MXenes could lead to better agreement with experiment.

| MXene | Experimental CLBE[33] / eV | Estimated CLBE / eV |
|---|---|---|
| **$Ti_2C(T_x)$** | 281.9 | 290.0 |
| **$V_2C(T_x)$** | 282.4 | 290.4 |
| **$Nb_2C(T_x)$** | 282.0 | 291.0 |
| **$Mo_2C(T_x)$** | 282.6 | 291.5 |

Table 7. Comparison between experimental absolute values of C(1s) CLBE of functionalized $M_2CT_x$ MXenes and estimated absolute C(1s) CLBEs of bare $M_2C$ MXenes.

# 8. CONCLUSIONS

In the present study, bare $M_2C$ (M= Ti, V, Cr, Zr, Nb, Mo, Hf, Ta, and W) MXene carbides have been investigated based on first-principles calculations to analyse the C(1s) CLBE. The main conclusions are summarized in the following points:

- The charge of the C atom Q(C) decreases when moving through the period along the early transition metals. The observed trend is reasonable attending to the electronegativities of metals, which increases in the same way.
- The C(1s) CLBEs increase through the periods of early transition metals. This trend is directly connected with the Q(C). The MXenes with a high accumulated charge on the C atom show low C(1s) CLBE and vice-versa.
- Connected to the previous trend, a nice correlation has been found between Q(C) and ΔCLBEs regardless the approximations used. This confirms that Q(C) has an important contribution determining the ΔCLBEs.
- Comparing the initial and final states, the initial state approach reports the best linear fitting, that is an indication of the main information obtained from BEs is presented in the neutral system and reinforces once again the usefulness of the separation of initial and final states.
- Finally, the general trends of calculated C(1s) CLBEs in bare $M_2C$ MXenes match well with experiments of functionalized $M_2CT_x$ MXenes with similar stoichiometry.

# 9. REFERENCES AND NOTES


1. Naguib, M.; Kurtoglu, M.; Presser, V.; Niu, J.; Heon, M.; Hultman, L.; Gogotsi, Y.; Barsoum M. W. Two-Dimensional Nanocrystals Produced by Exfoliation of $Ti_3AlC_2$. *Adv. Mater.* **2011**, *23*, 4248-4253.
2. Gogotsi, Y.; Anasori, B. The Rise of MXenes. *Acs. Nano.* **2019**, *13*, 8491-8494.
3. Jin-Cheng, L.; Xu, Z; Zhen, Z. Recent advances in MXene: Preparation, properties and applications. *Front. Phys*. **2015**, *10*, 107303.
4. Khazaei, M.; Mishra, A.; Venkataramanan, N.S.; Singh, A.K.; Yukoni, S. Recent advances in MXenes: from fundamentals to applications. Curr. Opin. Solid. State. Mater. Sci. **2019**, *23*(3)*,* 164–178.
5. Persson I, Halim J, Lind H, et al. 2D Transition Metal Carbides (MXenes) for Carbon Capture. *Av. Mater.* **2018**, *31*(2), 1805472.
6. Ihsanullah, I., MXenes (two-dimensional metal carbides) as emerging nanomaterials for water purification: Progress, challenges and prospects, *Chem. Eng. J.* **2020**, *388*, 124340.
7. Verger, L.; Natu, V.; Carey, M.; Barsoum, M. W. (n.d.). MXenes: An Introduction of Their Synthesis, Select Properties, and Applications. *Trends Chem.* **2019**, *1*(7), 656–669.
8. Anasori, B., Lukatskaya, M. R., & Gogotsi, Y. 2D metal carbides and nitrides (MXenes) for energy storage. *Nat. Rev. Mater.* **2017**, *2*(2), 17.
9. Bu, F.; Zagho, M.M.; Ibrahim, Y.; et al. Porous MXenes: Synthesis, structures, and applications. *Nano Today*. **2020**, *30*.
10. Pueyo, N.; Viñes, F.; Hieringer, W.; Illas, F. Predicting Core Level Binding Energies Shifts: Suitability of the Projector Augmented Wave Approach as Implemented in VASP. *J. Comput. Chem.* ***2017***, *38*(8), 518–522.
11. Viñes, F.; Sousa, C.; Illas, F. On the prediction of core level binding energies in molecules, surfaces and sòlids. *Phys. Chem. Chem. Phys.* **2018**, *20*(13), 8403–8410.
12. Jecko, T. On the Mathematical treatment of the Born-Oppenheimer approximation. *J. Math. Phys.* **2014,** *55*(5), 053504.
13. Levine, I. N. *Química cuántica*, 5th ed. Pearsons Educación, S.A.: Madrid, 2001.
14. Capelle K. A bird's-eye view of density-functional theory. *Braz. J. Phys.* **2002,** *36*(4a), 1318–1343.
15. Kohn, W.; Sham, L. J., Self-Consistent Equations Including Exchange and Correlation Effects. *Phys. Rev.,* **1965,** *140*, 4A.
16. Zhou A. A mathematical aspect of Hohenberg-Kohn theorem. *Sci. China. Math*. **2019**, *62*(1):63-68.
17. Hohenberg, P., Kohn, W., Inhomogeneous electron gas. *Phys. Rev*. **1964**, *136*, B864.
18. Perdew, JP., Burke K., Ernzerhof M. Generalized gradient approximation made simple. *Phys. Rev. Lett.* **1996**, *77*(18), 3865-3868.
19. Makov, G., & Payne, M. C. Periodic boundary conditions in ab initio calculations. *Phys. Rev. B*. **1995**, *51*(7), 4014–4022
20. Sousa, C., Tosoni, S., & Illas, F. Theoretical Approaches to Excited-State-Related Phenomena in Oxide Surfaces. *Chem. Rev.* **2013**, *113*(6), 4456–4495.
21. Kumar PSV, Raghavendra V, Subramanian V. Bader's Theory of Atoms in Molecules (AIM) and its Applications to Chemical Bonding. *J. Chem Sci*. **2016**, 128(10):1527-1536.
22. Wilson, T. R., & Eberhart, M. E. The Quantum Theory of Atoms in Molecules in Condensed Charge Density Space. *Can. J. Chem.* **2019**, *97*(11), 757–762.

23. Pueyo Bellafont, N., Vines, F., & Illas, F. Performance of the TPSS Functional on Predicting Core Level Binding Energies of Main Group Elements Containing Molecules: A Good Choice for Molecules Adsorbed on Metal Surfaces. *J. Chem. Theory. Comput*. **2016**, *12*(1), 324–331.
24. Bagus, P. S., Ilton, E. S., & Nelin, C. J. The interpretation of XPS spectra: Insights into materials properties. *Surf. Sci. Re*. **2013**, 68(2), 273–304.
25. Bellafont, N. P., Illas, F., & Bagus, P. S. Validation of Koopmans' theorem for density functional theory binding energies. *Phys. Chem. Chem. Phys*. **2015**, 17(6), 4015–4019.
26. Blöchl, P. E., Först, C. J., & Schimpl, J. The Projector Augmented Wave Method: ab-initio molecular dynamics with full wave functions. *Bull. Mater. Sci.* **2002**, *26*(1), 33–41.
27. Bellafont, N. P., Bagus, P. S., & Illas, F. Prediction of core level binding energies in density functional theory: Rigorous definition of initial and final state contributions and implications on the physical meaning of Kohn-Sham energies. *J. Chem. Phys*. **2015**, *142*(21), 1.
28. Baerends, E. J. On derivatives of the energy with respect to total electron number and orbital occupation numbers. A critique of Janak's theorem. *Mol. Phys.* **2019**, *118*(5).
29. Lang, N. D., Kohn, W. Theory of Metal Surfaces: Charge Density and Surface Energy. Phys. Rev. B. **1970**, *1*(12), 4555.
30. Kahn, A. Fermi level, work function and vacuum level. *Mater. Horiz.* **2016**, *3*(1), 7–10.
31. WebElements, https://www.webelements.com. (accessed May 29, 2020).
32. Greczynski, G., and Hultman, L. Compromising Science by Ignorant Instrument Calibration—Need to Revisit Half a Century of Published XPS Data. *Angew. Chem. Int. Ed.* **2020**, *59*(13), 5002–5006.
33. Halim, J. PhD. Thesis, Drexler University, 2016.

# 10. ACRONYMS

XPS: X-ray Photoelectron Spectroscopy

DFT: Density Functional Theory

BE: Binding Energy

CLBE: Core Level Binding Energy

ΔCLBE: Core Level Binding Energy shift

BOA: Born-Oppenheimer Approximation

HF: Hartree-Fock

CI: Configuration Interaction

KS: Kohn-Sham

xc: exchange correlation

LDA: Local Density Approximation

GGA: Generalized Gradient Approximation

PBE: Perdew–Burke–Ernzerhof

QTAIM: Quantum Theory of Atoms In Molecules

PAW: Projector Augmented Wave

IS: Initial State

FS: Final State

*fs*: Final State approach placing an electron in the conduction band

JS: Janak-Slater approach placing a half electron in the conduction band

$fs^n$: Final State approach placing an electron in the vacuum

$JS^n$: Janak-Slater approach placing a half electron in the vacuum

VASP: *Vienna ab initio Simulation*